

Indirect and monojet constraints on scalar leptoquarksAlexandre Alves,^{1,*} Oscar J. P. Éboli,^{2,†} Giovanni Grilli di Cortona,^{2,3,‡} and Roberto R. Moreira^{2,§}¹*Departamento de Física, Universidade Federal de São Paulo, UNIFESP, Diadema, 09972-270 São Paulo, Brazil*²*Instituto de Física, Universidade de São Paulo, 05508-090 São Paulo, Brazil*³*Institute of Theoretical Physics, Faculty of Physics, University of Warsaw, ul. Pasteura 5, PL-02-093 Warsaw, Poland*

(Received 14 January 2019; published 10 May 2019)

We obtain constraints on first- and second-generation scalar leptoquarks using the available data on dilepton (Drell-Yan) and monojet searches at the CERN Large Hadron Collider. Assuming that the leptoquark interactions respect the Standard Model gauge symmetries as well as lepton and baryon numbers, we show that the study of dilepton production enlarges the exclusion region on the mass and coupling plane with respect to the pair production searches for first-generation leptoquarks. Moreover, the monojet channel leads to a larger excluded parameter region for moderate to large values of the leptoquark Yukawa coupling than the presently available experimental results.

DOI: [10.1103/PhysRevD.99.095005](https://doi.org/10.1103/PhysRevD.99.095005)**I. INTRODUCTION**

The CERN Large Hadron Collider (LHC) has gathered a large amount of data that has been used not only to probe the Standard Model (SM), but also to look for new physics. The SM does not have any state that couples to leptoquark pairs; therefore, the discovery of such a state would be an indubitable sign of physics beyond the SM. In fact this is an ongoing search by the LHC collaborations; see, for instance, Refs. [1,2].

Leptoquarks are particles which interact with quark-lepton pairs. They appear in a plethora of models where quarks and leptons are treated on the same footing. The first appearance of leptoquarks was in the Pati-Salam model [3,4] and they are also present in grand unified theories [5], composite models [6], or in supersymmetric models with violation of R parity [7]. Leptoquarks modify the low-energy physics which, in turn, leads to constraints on their masses and couplings. For instance, leptoquarks might contribute to the decay of mesons [8], induce flavor-changing neutral currents (FCNCs) [4,8], give rise to lepton-flavor-violating decays [9], and contribute to the radiative correction to Z physics [10,11]. Recently some

anomalies were observed that point towards lepton flavor universality violation in neutral- and charged-current processes [12–21]. One possible explanation for the departures from the SM is the existence of leptoquarks with masses $\mathcal{O}(\text{TeV})$; see, for instance, Refs. [22–37] and references therein.

Since leptoquarks carry color, they can be pair produced via QCD [38] at the LHC and the main advantage of this channel is that the production cross section depends only on the leptoquark mass. Presently most of the LHC searches for leptoquarks are based on their pair production. The LHC RUN 1 data excludes first- (second-)generation scalar leptoquarks with masses smaller than 1050 (1080) GeV [39,40] provided the leptoquark decays exclusively into a charged lepton and a jet. The already available results from LHC Run 2 expands these limits to 1435 and 1520 GeV for first- and second-generation leptoquarks, respectively [2,41].

Leptoquarks can also be produced singly in association with a lepton through its coupling to a quark-lepton pair [42–45]. In fact, this process has a larger phase space than the leptoquark pair production and for $\mathcal{O}(1)$ couplings and 100% branching ratio into a charged lepton plus an up quark, the bounds [$\mathcal{O}(1.3\text{--}1.7)$ TeV] from the Run 1 data of the LHC can be even stronger than the pair production ones [46]. At the LHC it is also possible to look for indirect signs of leptoquarks in the production of charged lepton pairs [42,45,47,48].

Leptoquarks coupling to a neutrino and a quark give rise to monojet events due to their single production. In this case, the leptoquark decay leads to a hard missing transverse energy spectrum peaking around half the leptoquark

* aalves.unifesp@gmail.com† eboli@if.usp.br‡ ggrillidc@fuw.edu.pl§ robertor@fma.if.usp.br

mass. It is interesting to notice that models where leptoquarks couple to dark matter [49] with sizable branching ratios could also be constrained by these monojet searches. At the same time they alleviate other constraints due to the diminished leptoquark branching ratio to an SM lepton plus a quark. Moreover, the LHC collaborations also searched for leptoquarks in the monobottom [50–52] and monotop quark [53,54] channels which have been explored in the search for dark matter. These channels constitute alternatives to pair production in the case where the third-generation leptoquarks are too heavy.

If leptoquarks are too heavy to be pair produced at the LHC, single production and indirect effects in lepton pair production remain as alternatives to search for these particles [42]. In this work we study the attainable bounds on first- and second-generation scalar leptoquarks using the available data on lepton pair production and the monojet searches for dark matter [55]. Our results depend on the leptoquark mass as well as its Yukawa coupling to quark-lepton pairs. As a consequence, they will yield more information on the leptoquark properties if a signal is observed, complementing the leptoquark pair production searches. We show that the study of dilepton production enlarges the exclusion region in the plane mass and coupling with respect to the pair production searches. Additionally, the monojet channel for first-generation leptoquarks also leads to a larger exclusion region than the canonical $\ell^+\ell^-jj$ and $\ell^\pm\nu jj$ (with $\ell = e$ and μ) topologies for moderate and large values of the leptoquark Yukawa coupling. The monojet channel is also able to probe a larger fraction of the parameter space than the jjE_T^{miss} final state [56].

II. ANALYSES FRAMEWORK

In order to describe the leptoquark interactions at the presently available energies we assume that leptoquarks are the only accessible states from an extension of the SM. Moreover, we impose that their interactions respect the SM gauge symmetry $SU(3)_c \otimes SU(2)_L \otimes U(1)_Y$. Furthermore, due to the stringent bounds coming from proton lifetime experiments the leptoquark interactions are required to respect baryon and lepton numbers. Within these hypotheses, there are five distinct possibilities for scalar leptoquarks [57]: two $SU(2)_L$ singlet states (S_1 and \tilde{S}_1), two doublet states (R_2 and \tilde{R}_2) and one triplet (S_3), whose interactions with quarks and leptons are

$$\begin{aligned} \mathcal{L}_{\text{eff}} = & (g_{1L}\bar{q}_L^c i\tau_2 \ell_L + g_{1R}\bar{u}_R^c e_R)S_1 + \tilde{g}_{1R}\bar{d}_R^c e_R \tilde{S}_1 \\ & + g_{3L}\bar{q}_L^c i\tau_2 \vec{\tau} \ell_L \cdot \vec{S}_3 + h_{2L}R_2^T \bar{u}_R i\tau_2 \ell_L \\ & + h_{2R}\bar{q}_L e_R R_2 + \tilde{h}_{2L}\tilde{R}_2^T \bar{d}_R i\tau_2 \ell_L, \end{aligned} \quad (2.1)$$

where q_L (ℓ_L) stands for the left-handed quark (lepton) doublet, u_R , d_R , and e_R are the singlet components of the fermions, τ_i are the Pauli matrices, and we denote the charge-conjugated fermion fields by $\psi^c = C\bar{\psi}^T$. Moreover, we omit

the flavor indices of the fermions. The couplings of the leptoquarks to the electroweak gauge bosons are determined by the $SU(3)_c \otimes SU(2)_L \otimes U(1)_Y$ gauge invariance.

At low energies, leptoquarks give rise to FCNC processes [4,8,58] that are very constrained. In order to avoid stringent bounds, we assume that the scalar leptoquarks couple only to a single generation of quarks and just one of leptons. In fact, we consider that the leptoquarks interact with the same generation of quarks and leptons. Notwithstanding, there is a residual amount of FCNC due to the mixing in the quark sector that leads to bounds on leptoquark couplings to the first two generations [59,60]. Moreover, data on decays of pseudoscalar mesons, like the pions, put stringent bounds on leptoquarks unless their couplings are chiral—that is, they are either left- or right-handed [8,59,60]. As a rule of a thumb, the low-energy data constrain first-generation-leptoquark masses to be larger than 0.5–1.0 TeV for leptoquark Yukawa couplings of the order of the proton charge e [61].

In our analysis we focus on leptoquarks that conserve fermion number $F = 3B + L$, i.e., the states R_2 and \tilde{R}_2 . For the sake of simplicity, we assume that leptoquarks belonging to a given $SU(2)_L$ multiplet are degenerate. We study the following scenarios that satisfy the described low-energy bounds:

- (1) \tilde{R}_2 coupling only to the first generation, i.e., only to down quarks, electrons and its neutrino. We label this scenario as \tilde{R}_2^d .
- (2) R_2 coupled to the first generation and exhibiting only left-handed interactions ($h_{2R} = 0$). In this case the leptoquarks interact with up quarks, electrons and the respective neutrino. We refer to this scenario as R_2^L .
- (3) \tilde{R}_2 coupling only to the second generation—that is to strange quarks, muons and the corresponding neutrinos. We call this scenario \tilde{R}_2^s .

These scenarios allows us to obtain bounds on other leptoquarks. For instance, the constraints on R_2 (second scenario) originating from the dilepton data can be easily translated into bounds on the singlet S_1 or the third component of the triplet \tilde{S}_3 . On the other hand, the dilepton limits in the first scenario can be readily transposed to \tilde{S}_1 and one component of \tilde{S}_3 . Furthermore, the \tilde{R}_2^s case is the one leading to the strongest constraints on second-generation leptoquarks.

In order to study leptoquarks at the LHC we consider their indirect effects in Drell-Yan processes [42]

$$pp \rightarrow e^+e^-/\mu^+\mu^- + X \quad (2.2)$$

as well as in monojet searches

$$pp \rightarrow j + E_T^{\text{miss}}. \quad (2.3)$$

In the Drell-Yan 8 TeV analyses we use the data in Ref. [62] that contain the e^+e^- and $\mu^+\mu^-$ invariant

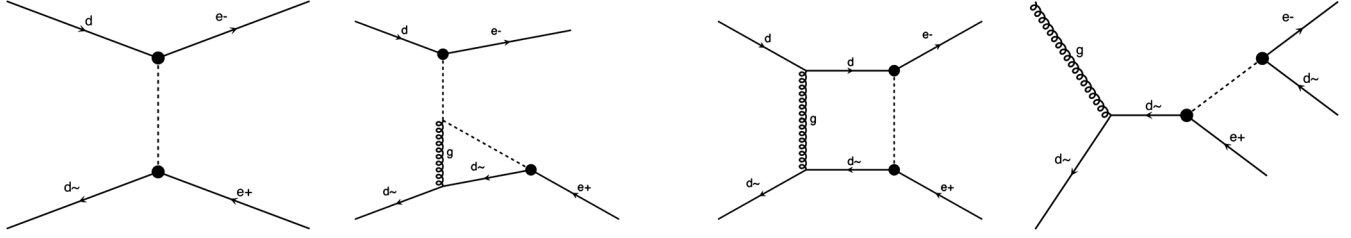


FIG. 1. Sample of diagrams generated by MADGRAPH5_AMC@NLO in the NLO evaluation of the Drell-Yan production. The leptoquark is represented by the dashed line.

mass distribution in the fiducial region defined by the leading (subleading) lepton having $p_T^\ell > 40$ GeV (30 GeV) and both leptons within the rapidity range $|\eta| < 2.5$. These results are given at the QED Born level which simplifies the comparison with the leptoquark

predictions. Since the 13 TeV Drell-Yan analyses have not been released by ATLAS and CMS we use the data on searches for new resonances decaying into lepton pairs given in Refs. [63,64]. More specifically, the data we use is¹

Channel	Kinematical range	# bins	Int. Lum.	Data set
e^+e^-	$116 < m_{ee} < 1500$ GeV	12	20.3 fb^{-1}	ATLAS 8 TeV [62] Table 6
$\mu^+\mu^-$	$116 < m_{\mu\mu} < 1500$ GeV	12	20.3 fb^{-1}	ATLAS 8 TeV [62] Table 9
e^+e^-	$80 < m_{ee} < 6000$ GeV	9	36.1 fb^{-1}	ATLAS 13 TeV [63] Table 6
$\mu^+\mu^-$	$80 < m_{\mu\mu} < 6000$ GeV	9	36.1 fb^{-1}	ATLAS 13 TeV [63] Table 7
e^+e^-	$120 < m_{ee} < 1800_+$ GeV	6	$36. \text{ fb}^{-1}$	CMS 13 TeV [64] Table 2
$\mu^+\mu^-$	$120 < m_{\mu\mu} < 1800_+$ GeV	6	$36. \text{ fb}^{-1}$	CMS 13 TeV [64] Table 3

As for the monojet analysis, we use the CMS results [55] at 13 TeV with an integrated luminosity of 35.9 fb^{-1} . The CMS analysis is done as a counting experiment in 22 independent signal regions satisfying $E_T^{\text{miss}} > 250$ GeV, $p_T^{\text{jet}} > 100$ GeV and $|\eta_j| < 4.5$. For each of the above experiments and channels, we extract from the experimental publications the observed event rates in each bin N_{obs}^i , the background expectations N_{bkg}^i , and the SM predictions N_{SM}^i , as well as the statistical and systematic errors.

In order to confront the leptoquark predictions with the available data, first we simulate the processes (2.2) and (2.3) using MADGRAPH5_AMC@NLO [65] with the UFO files for our effective lagrangian generated with FEYNRULES [66,67]. The counterterms needed for the next-to-leading-order (NLO) evaluation of the Drell-Yan process are evaluated using the package NLOCT [68]. Moreover, in NLO calculations, MADGRAPH5_AMC@NLO automatically includes not only the SM one-loop and real emission contributions, but also the t -channel leptoquark exchange at tree level (see the first diagram of Fig. 1), as well as the virtual corrections involving leptoquarks (as in the second and third diagrams in

Fig. 1) and its contribution to the real emission (last diagram of Fig. 1). For further details, see Refs. [69,70].

The 8 TeV Drell-Yan simulation is carried out in next-to-leading-order QCD at the parton level while the 13 TeV dilepton analyses are done at leading order using PYTHIA [71] to perform the parton shower, while the fast detector simulation is carried out with DELPHES [72]. In the jet plus missing transverse momentum analysis we merge the Monte Carlo simulations containing zero, one and two jets and perform the jet matching. In order to account for higher-order corrections and additional detector effects we normalize bin by bin our dilepton simulations to the corresponding ones performed by the experimental collaborations. Then we apply these correction factors to our simulated distributions taking into account the leptoquark contributions.

In order to perform the statistical analysis we define a χ^2 function for the dilepton analysis given by²

$$\chi_{\ell\ell}^2(m_R, \lambda) = \sum_i \frac{(N_{\text{sig}}^i(m_R, \lambda) + N_{\text{bkg}}^i - N_{\text{obs}}^i)^2}{N_{\text{obs}}^i + \sigma_{\text{bkg}}^2}, \quad (2.4)$$

¹We merged the two last bins in Ref. [63] to ensure Gaussianity. The last bin of Ref. [64] (denoted by 1800_+) is for $m_{ee}(m_{\mu\mu}) > 1800$ GeV.

²In the Drell-Yan analysis, we estimate the effect of the systematic uncertainties by means of a simplified treatment in terms of two pulls [73,74].

where N_{sig} are the signal events obtained for the different models using the corrections factors and σ_{bkg}^i are the uncertainties on the background obtained by the experiments. Here $m_R(\lambda)$ stands for the leptoquark mass (Yukawa coupling). On the other hand, for the monojet searches we use a Gaussian likelihood containing the correlation between the different bins obtained in Ref. [55]

$$\chi_{\text{monojet}}^2(m_R, \lambda) = \sum_{i,j} (N_{\text{sig}}^i(m_R, \lambda) + N_{\text{bkg}}^i - N_{\text{obs}}^i)(\sigma^2)_{ij}^{-1} \times (N_{\text{sig}}^j(m_R, \lambda) + N_{\text{bkg}}^j - N_{\text{obs}}^j), \quad (2.5)$$

where $\sigma_i^2 = \sigma_i \rho_{ij} \sigma_j$ and ρ is the correlation matrix. Finally, the combined results are obtained with the following χ^2 :

$$\chi_{\text{combined}}^2(m_R, \lambda) = \sum_i \chi_i^2(m_R, \lambda), \quad (2.6)$$

where i runs over the different searches (Drell-Yan, dilepton and monojet).

III. RESULTS

We start our analyses considering the first-generation scenarios. In Fig. 2 we present the results of our analyses for the \tilde{R}_2^d case. The left panel of this figure depicts the excluded regions at 95% C.L. for each of the four data sets described in the previous section. The shaded purple region on the left of the curve is excluded by the Drell-Yan analysis of the ATLAS 8 TeV search. The blue area is excluded by the CMS monojet analysis at 13 TeV, while the

CMS and ATLAS dilepton analysis of 13 TeV data exclude the yellow and red regions, respectively. Finally, for the sake of comparison, the solid and dashed black lines show the exclusion from the pair production experimental searches at 8 and 13 TeV, respectively. As we can see, the most stringent limits from masses above 1 TeV originate from the ATLAS data on the search for new resonances decaying into e^+e^- pairs [63]. On the other hand, in the low-mass region ($\simeq 1$ TeV) the monojet data leads to stronger limits on the leptoquark \tilde{R}_2 than the dilepton analysis.

When we combine the three data sets on dileptons, as shown by the dashed blue curve in the right panel of Fig. 2, we see that the bounds are basically due to the ATLAS 13 TeV data on dileptons, except for masses smaller than 700 GeV where the stronger limits come from the 8 TeV Drell-Yan analysis. Furthermore, the inclusion of the monojet data in the combined χ^2 strengthens the limits for low leptoquark masses, as shown by the solid blue curve. It is important to keep in mind that the combination of dilepton and monojet constraints is only possible because we assumed that the leptoquarks belonging to the multiplet \tilde{R}_2 are degenerate.

We expect stronger constraints on the R_2^l scenario than on the \tilde{R}_2^d one since the former couples to up quarks while the latter couples to down quarks. This indeed happens as shown in Fig. 3. In the left panel the purple, blue, yellow and red shaded regions correspond respectively to 95% C.L. limits from 8 TeV ATLAS Drell-Yan, 13 TeV CMS monojet, 13 TeV CMS dilepton and 13 TeV ATLAS dilepton searches. Moreover, the black solid and dashed

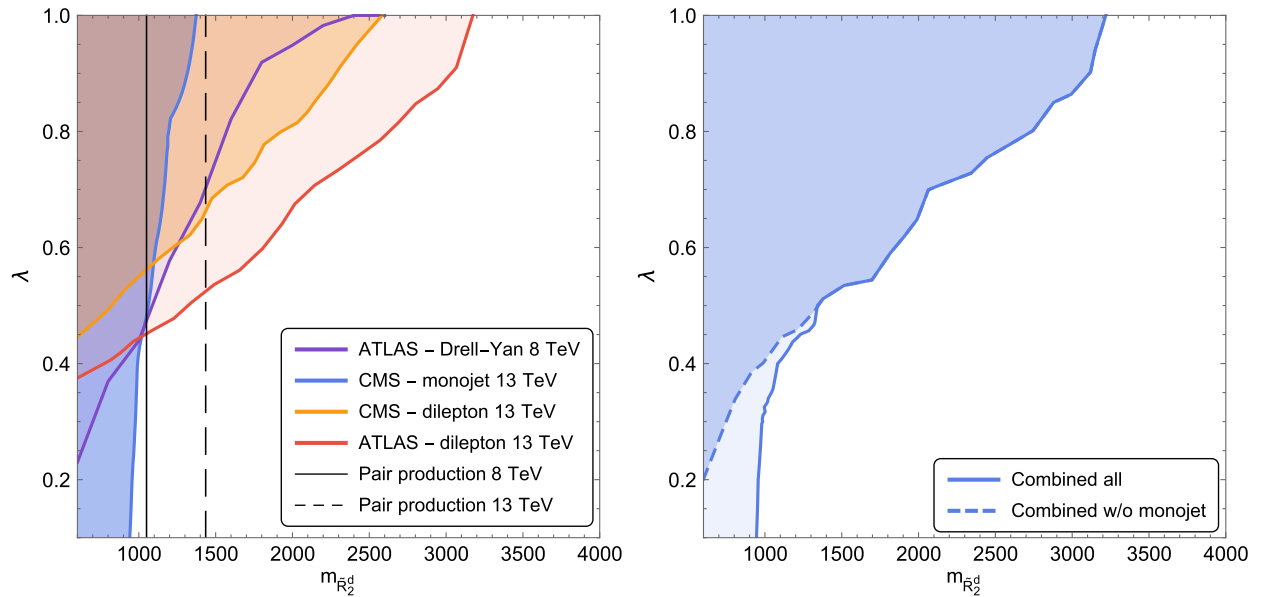


FIG. 2. Excluded regions at 95% C.L. for the \tilde{R}_2^d scenario. Left: Limits from the ATLAS Drell-Yan search at 8 TeV (purple) [62], the CMS monojet search at 13 TeV (blue) [55], the CMS and ATLAS dilepton searches at 13 TeV (yellow and red, respectively) [63,64], and the pair production experimental searches at 8 and 13 TeV (black solid and black dashed, respectively) [2,39–41]. Right: Combined limits including all searches (solid blue) and excluding only the monojet one (dashed blue).

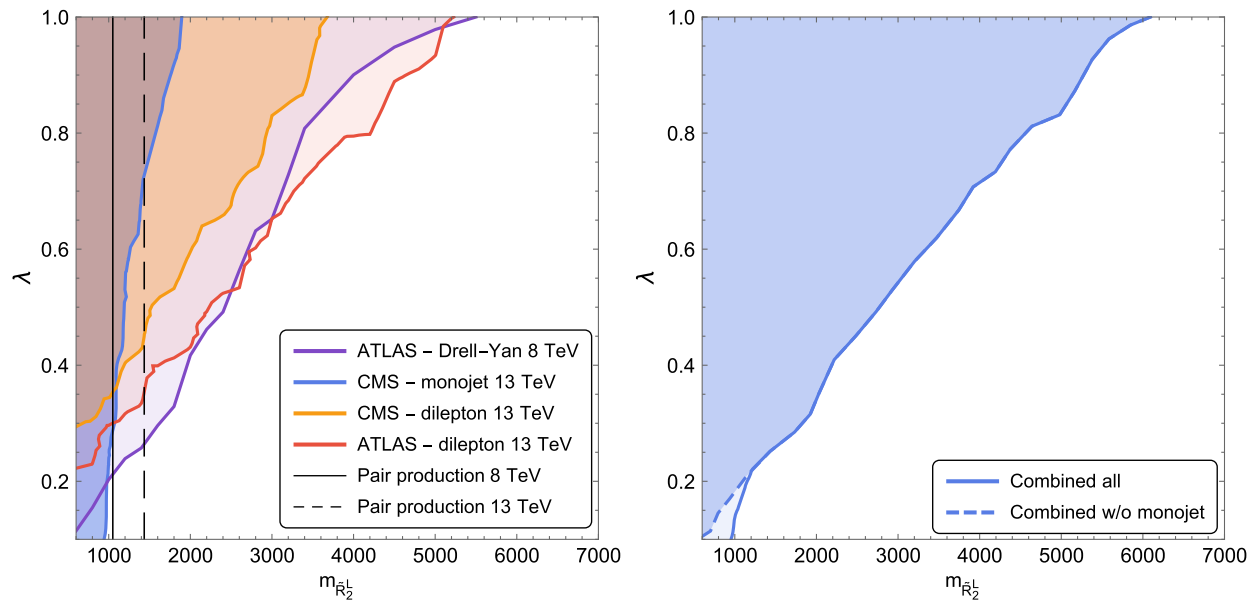


FIG. 3. Excluded regions at 95% C.L. for the R_2^I scenario. Left: Limits from the ATLAS Drell-Yan search at 8 TeV (purple) [62], the CMS monojet search at 13 TeV (blue) [55], the CMS and ATLAS dilepton searches at 13 TeV (yellow and red, respectively) [63,64], and the pair production experimental searches at 8 and 13 TeV (black solid and black dashed, respectively) [2,39–41]. Right: Combined limits including all searches (solid blue) and excluding only the monojet one (dashed blue).

lines denote the 95% C.L. experimental constraints from pair production at 8 and 13 TeV.

We learn from the left panel of this figure that for masses below 1 TeV the monojet data give rise to tighter bounds than the dilepton study. On the other hand, for larger masses the ATLAS dilepton data at 13 TeV and the ATLAS 8 TeV Drell-Yan data lead to similar constraints. Despite the lower integrated luminosity and energy the 8 TeV Drell-Yan limits are similar to the 13 TeV ones since the Drell-Yan cuts and presentation of the data are more suitable for the present study.

The right panel of Fig. 3 contains the limits obtained by combining the dilepton data sets only (dashed blue curve) as well as limits including the monojet one (solid blue line). In this scenario, the combined dilepton bounds are tighter than the separate limits. Moreover, the inclusion of the monojet data gives rise to stronger limits for masses below 1 TeV.

The scenario \tilde{R}_2^s provides the strongest limits on second generation leptoquarks due to its coupling to strange quarks. We display in Fig. 4 the results for this scenario, with the same color coding as in the previous figures. The most stringent dilepton limits come from the 8 TeV Drell-Yan analysis with the ATLAS and CMS 13 TeV data leading to similar weaker constraints; see the left panel of this figure. Moreover, the impact of the monojet is similar to the ones of the other cases: the monojet data leads to the best bounds for small to moderate Yukawa couplings, due to the small dilepton cross section at small couplings. This fact can be clearly seen in the left panel of this figure which depicts the results from combining only the dilepton

searches (blue dashed curve) or including the monojet data set (solid blue line). The left panel shows also that, for this scenario, the pair production searches still give the strongest constraints.

IV. DISCUSSION

The indirect leptoquark signal in the Drell-Yan process is complementary to the pair production searches since it is able to probe higher leptoquark masses. On the other hand, the indirect analysis requires the introduction of the unknown leptoquark Yukawa coupling. To illustrate this point let us focus on the 8 TeV data and first-generation leptoquarks. From the left panel of Fig. 2 we see that the analysis of indirect effects on the Drell-Yan production expands the excluded region by the pair production search for Yukawa couplings $\lambda \gtrsim 0.5$. In fact, the 8 TeV indirect limits are still more stringent than the direct searches at 13 TeV for Yukawa couplings $\lambda \gtrsim 0.7$. Moreover, when we consider all available 13 TeV data, the indirect limits are stronger than the pair production ones for Yukawa couplings $\lambda \gtrsim 0.5$ and extend the exclusion region to leptoquark masses of the order of 3.5 TeV if the leptoquark Yukawa coupling is $\lambda \sim 1$.

The importance of the indirect effects is even more dramatic when we consider the R_2^I scenario where the scalar leptoquark couples to up quarks. Indeed, Fig. 3 shows that the 8 TeV Drell-Yan limits are more stringent than the presently available 13 TeV direct search limits for Yukawa couplings $\lambda \gtrsim 0.25$. In addition, the combined 8 and 13 TeV dilepton data allow the exclusion of leptoquarks with mass smaller

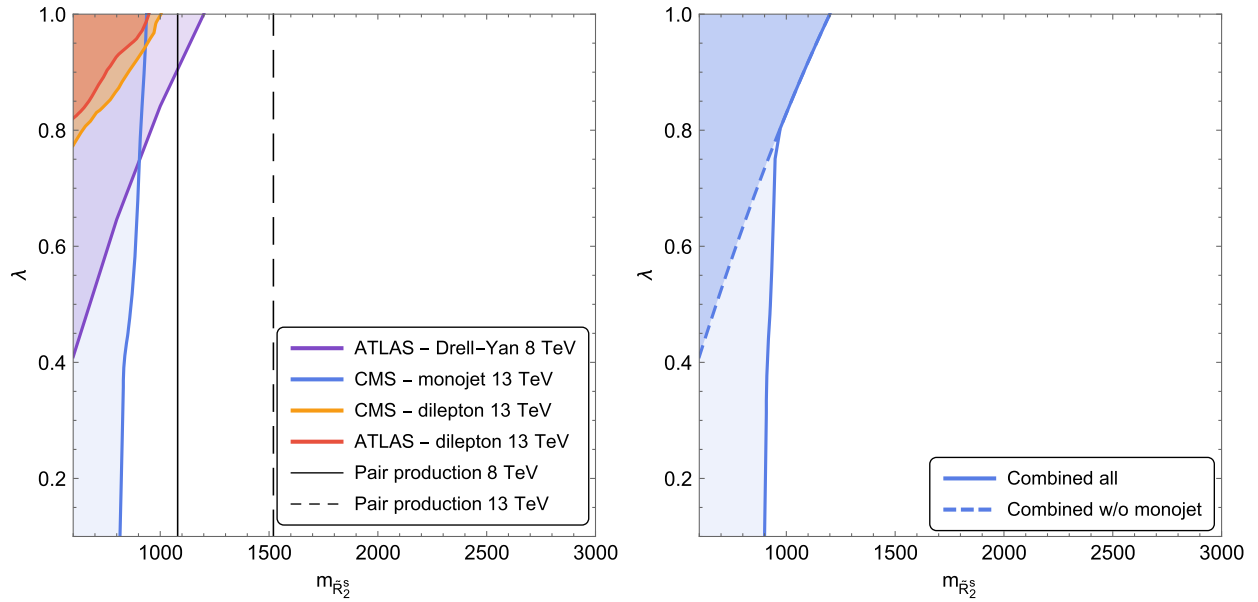


FIG. 4. Excluded regions at 95% C.L. for the \tilde{R}_2^s scenario. Left: Limits from the ATLAS Drell-Yan search at 8 TeV (purple) [62], the CMS monojet search at 13 TeV (blue) [55], the CMS and ATLAS dilepton searches at 13 TeV (yellow and red, respectively) [63,64], and the pair production experimental searches at 8 and 13 TeV (black solid and black dashed, respectively) [2,39–41]. Right: Combined limits including all searches (solid blue) and excluding only the monojet one (dashed blue).

than 7 TeV provided the Yukawa coupling is $\lambda \sim 1$. In the case of second-generation leptoquarks, scenario \tilde{R}_2^s , the impact of the leptoquarks in the dilepton invariant mass spectrum is much smaller due to its coupling to strange quarks. Therefore, the indirect limits turn out to be milder than the pair production ones that proceed through strong interactions; see Fig. 4.

At this point it is interesting to compare our findings with previous works that analyzed indirect effects of leptoquarks at the LHC. For very large leptoquark masses their exchange in the t -channel can be encoded by a four-fermion dimension-six operator [75–77]. This method has two shortcomings since it does not properly take into account the leptoquark interference with the SM contribution, as well as, the leptoquark propagator [76]. In any case, the available limits using this procedure are much weaker than the ones presented here. These drawbacks can be mitigated with the addition of form factors to the four-fermion contact interactions [78] leading to similar results to the ones obtained here for the Run 1 data. However, for a specific model it is better to fit it directly to data, thus avoiding any ambiguity and also allowing the evaluation of higher-order corrections.

Our monojet analyses lead to limits that complement the dilepton studies at low leptoquark masses (smaller than 1 TeV). For large Yukawa coupling, e.g., $\lambda \sim 1$, the monojet analysis excludes leptoquarks with masses up to 2 TeV (950 GeV) for first- (second-)generation leptoquarks. Notwithstanding, for this region of Yukawa couplings the indirect dilepton process leads to much stronger constraints. Furthermore, our results indicate that the

monojet channel and the single production of leptoquarks decaying into a charged lepton and a jet [46] have similar capabilities to search for these particles. On the other hand, for second-generation leptoquarks the monojet search is not competitive with respect to the dilepton analysis.

Confronting the monojet bounds on first-generation leptoquarks with ones originating from the ongoing studies of the $\ell^+\ell^-jj$ and $\ell^\pm\nu jj$ topologies [2], we learn that the monojet search leads to tighter bounds than these pair production searches only for Yukawa couplings $\lambda \gtrsim 0.7$ in the \tilde{R}_2^L scenario. Furthermore, our results show that the monojet channel extends considerably the exclusion limits originating from leptoquark pair production followed by their decay into a jet and a neutrino, i.e., the jjE_T^{miss} channel [56].

We can also abandon the hypothesis of the degeneracy of leptoquarks belonging to the same multiplet if we consider separately the dilepton and monojet constraints. In this case, we have to examine the couplings of each component of the leptoquark multiplets:

- (1) The dilepton bounds on \tilde{R}_2^d apply to all leptoquarks that couple to electrons and down quarks, that is, \tilde{S}_1 , the components 1 and 2 of \tilde{S}_3 , the down component of R_2 with right-handed couplings, and the up component of \tilde{R}_2^d (of course).
- (2) The dilepton constraints on R_2 are the same for S_1 , the third component of \tilde{S}_3 and the up (down) component of R_2 with left-handed (right-handed) coupling.
- (3) The monojet analyses labeled \tilde{R}_2^d are the same for S_1 , the third component of \tilde{S}_3 and the down component

of \tilde{R}_2^d . Our R_2^L monojet study is valid for the components 1 and 2 of \tilde{S}_3 and the down component of R_2 with left-handed couplings.

Finally, let us comment on models containing leptoquarks that address the anomalies observed in lepton flavor universality. In general (see for instance Ref. [27]), the proposed $\mathcal{O}(\text{TeV})$ leptoquarks mediate transitions between the second and third families due to strong $e - \mu$ conversion constraints. Our results for the \tilde{R}_2^s scenario indicate that indirect effects on the $\mu^+\mu^-$ production will not strengthen the direct pair searches for scalar leptoquarks. Some models also present vector leptoquarks. However, even the direct search limits on them depend upon two additional parameters needed to describe their $SU(3)_C$ gauge interactions, therefore rendering the analyses much more involved [79,80]. High- p_T observables involving the processes $pp \rightarrow \tau\tau$ and $pp \rightarrow \tau\mu$ are more sensitive to leptoquarks mediating interactions with the third generation which are also relevant to the observed B anomalies [81–83]. The relevant monojet channel, by its turn, might involve bottom jets and should benefit more from a dedicated analysis of b -tagged jets [50].

V. CONCLUSIONS

In this work, we have considered collider constraints on first- and second-generation leptoquarks. In particular, we studied the \tilde{R}_2 scalar leptoquark model with couplings only to the right-handed down (strange) quark and the first-(second-)generation lepton doublet, and the R_2 scalar leptoquark model with couplings only to the right-handed up quark and the first-generation left-handed lepton doublet. Stringent experimental bounds on leptoquarks come from their pair production followed by their prompt decays. This production mechanism is independent of the leptoquark Yukawa couplings. For large leptoquark Yukawa couplings, on the other hand, single production becomes important. This is especially relevant for couplings with the

first-generation quarks because of their large parton distribution functions.

Our results show the importance of the search for leptoquark effects in the Drell-Yan process since it allows to extend considerably the reach in leptoquark mass for moderate to large leptoquark Yukawa couplings. For example, the scalar \tilde{R}_2 (R_2) leptoquark model with couplings to the first-generation quark is excluded up to ~ 3.2 (~ 5.6) TeV for $\lambda \sim 1$, overcoming the pair production limits $\lesssim 1.5$ TeV. In addition, we showed that the monojet channel is a viable alternative to further probe leptoquarks. Moreover, should a signal arise at the LHC, these kind of processes would give more information on the leptoquark properties, given their dependence on the leptoquark mass and Yukawa coupling.

Finally, we discussed how to interpret the results obtained in this work if we abandon the hypothesis of degeneracy of the leptoquarks belonging to the same $SU(2)$ multiplet and the possible connection to constraints on the singlet (S_1) or each component of the triplet (S_3) scalar leptoquark models.

ACKNOWLEDGMENTS

This work is supported in part by Conselho Nacional de Desenvolvimento Científico e Tecnológico (CNPq) and by Fundação de Amparo à Pesquisa do Estado de São Paulo (FAPESP) Grant No. 2012/10095-7. A. A. thanks Conselho Nacional de Desenvolvimento Científico (CNPq) for its financial support (Grant No. 307265/2017-0). R. R. M. was supported by FAPESP process no. 2013/26511-1. G. G. d. C. has been supported by the FAPESP process no. 2016/17041-0 and by the National Science Centre, Poland, under research grant no. 2017/26/D/ST2/00225. G. G. d. C. would like to thank FAPESP Grant No. 2016/01343-7 for funding his visit to ICTP-SAIFR where part of this work was done.

-
- [1] M. Aaboud *et al.* (ATLAS Collaboration), *New J. Phys.* **18**, 093016 (2016).
 - [2] A. M. Sirunyan *et al.* (CMS Collaboration), *Phys. Rev. D* **99**, 052002 (2019).
 - [3] J. C. Pati and A. Salam, *Phys. Rev. D* **8**, 1240 (1973).
 - [4] J. C. Pati and A. Salam, *Phys. Rev. D* **10**, 275 (1974); **11**, 703(E) (1975).
 - [5] H. Georgi and S. L. Glashow, *Phys. Rev. Lett.* **32**, 438 (1974).
 - [6] B. Schrempp and F. Schrempp, *Phys. Lett.* **153B**, 101 (1985).
 - [7] R. Barbier *et al.*, *Phys. Rep.* **420**, 1 (2005).
 - [8] O. U. Shanker, *Nucl. Phys.* **B206**, 253 (1982).
 - [9] I. Dorsner, S. Fajfer, A. Greljo, J. F. Kamenik, and N. Kosnik, *Phys. Rep.* **641**, 1 (2016).
 - [10] J. K. Mizukoshi, O. J. P. Eboli, and M. C. Gonzalez-Garcia, *Nucl. Phys.* **B443**, 20 (1995).
 - [11] G. Bhattacharyya, J. R. Ellis, and K. Sridhar, *Phys. Lett. B* **336**, 100 (1994); **338**, 522(E) (1994).
 - [12] J. P. Lees *et al.* ((BABAR Collaboration), *Phys. Rev. Lett.* **109**, 101802 (2012).
 - [13] R. Aaij *et al.* (LHCb Collaboration), *Phys. Rev. Lett.* **115**, 111803 (2015); **115**, 159901(E) (2015).
 - [14] M. Huschle *et al.* (Belle Collaboration), *Phys. Rev. D* **92**, 072014 (2015).

- [15] Y. Sato *et al.* (Belle Collaboration), *Phys. Rev. D* **94**, 072007 (2016).
- [16] Y. Amhis *et al.* (HFLAV Collaboration), *Eur. Phys. J. C* **77**, 895 (2017).
- [17] R. Aaij *et al.* (LHCb Collaboration), *Phys. Rev. Lett.* **111**, 191801 (2013).
- [18] R. Aaij *et al.* (LHCb Collaboration), *J. High Energy Phys.* **02** (2016) 104.
- [19] M. Ciuchini, M. Fedele, E. Franco, S. Mishima, A. Paul, L. Silvestrini, and M. Valli, *J. High Energy Phys.* **06** (2016) 116.
- [20] R. Aaij *et al.* (LHCb Collaboration), *Phys. Rev. Lett.* **113**, 151601 (2014).
- [21] R. Aaij *et al.* (LHCb Collaboration), *J. High Energy Phys.* **08** (2017) 055.
- [22] I. Doršner, S. Fajfer, N. Košnik, and I. Nišandžić, *J. High Energy Phys.* **11** (2013) 084.
- [23] Y. Sakaki, M. Tanaka, A. Tayduganov, and R. Watanabe, *Phys. Rev. D* **88**, 094012 (2013).
- [24] L. Calibbi, A. Crivellin, and T. Ota, *Phys. Rev. Lett.* **115**, 181801 (2015).
- [25] M. Bauer and M. Neubert, *Phys. Rev. Lett.* **116**, 141802 (2016).
- [26] R. Barbieri, G. Isidori, A. Pattori, and F. Senia, *Eur. Phys. J. C* **76**, 67 (2016).
- [27] D. Becirevic, N. Kosnik, O. Sumensari, and R. Z. Funchal, *J. High Energy Phys.* **11** (2016) 035.
- [28] A. Crivellin, D. Müller, and T. Ota, *J. High Energy Phys.* **09** (2017) 040.
- [29] N. Assad, B. Fornal, and B. Grinstein, *Phys. Lett. B* **777**, 324 (2018).
- [30] L. Calibbi, A. Crivellin, and T. Li, *Phys. Rev. D* **98**, 115002 (2018).
- [31] M. Blanke and A. Crivellin, *Phys. Rev. Lett.* **121**, 011801 (2018).
- [32] A. Crivellin, C. Greub, F. Saturnino, and D. Müller, *Phys. Rev. Lett.* **122**, 011805 (2019).
- [33] A. Biswas, D. K. Ghosh, N. Ghosh, A. Shaw, and A. K. Swain, [arXiv:1808.04169](https://arxiv.org/abs/1808.04169).
- [34] T. Mandal, S. Mitra, and S. Raz, *Phys. Rev. D* **99**, 055028 (2019).
- [35] A. Biswas, A. K. Swain, and A. Shaw, [arXiv:1811.08887](https://arxiv.org/abs/1811.08887).
- [36] J. Aebischer, A. Crivellin, and C. Greub, *Phys. Rev. D* **99**, 055002 (2019).
- [37] B. Fornal, S. A. Gadam, and B. Grinstein, *Phys. Rev. D* **99**, 055025 (2019).
- [38] J. L. Hewett and S. Pakvasa, *Phys. Rev. D* **37**, 3165 (1988).
- [39] G. Aad *et al.* (ATLAS Collaboration), *Eur. Phys. J. C* **76**, 5 (2016).
- [40] V. Khachatryan *et al.* (CMS Collaboration), *Phys. Rev. D* **93**, 032004 (2016).
- [41] A. M. Sirunyan *et al.* (CMS Collaboration), *Phys. Rev. D* **99**, 032014 (2019).
- [42] O. J. P. Eboli and A. V. Olinto, *Phys. Rev. D* **38**, 3461 (1988).
- [43] T. Mandal, S. Mitra, and S. Seth, *J. High Energy Phys.* **07** (2015) 028.
- [44] S. Bansal, R. M. Capdevilla, A. Delgado, C. Kolda, A. Martin, and N. Raj, *Phys. Rev. D* **98**, 015037 (2018).
- [45] M. Schmaltz and Y.-M. Zhong, *J. High Energy Phys.* **01** (2019) 132.
- [46] V. Khachatryan *et al.* (CMS Collaboration), *Phys. Rev. D* **93**, 032005 (2016); **95**, 039906(E) (2017).
- [47] N. Raj, *Phys. Rev. D* **95**, 015011 (2017).
- [48] S. Bansal, A. Delgado, C. Kolda, and M. Quiros, [arXiv:1812.04232](https://arxiv.org/abs/1812.04232).
- [49] B. Allanach, A. Alves, F. S. Queiroz, K. Sinha, and A. Strumia, *Phys. Rev. D* **92**, 055023 (2015).
- [50] T. Lin, E. W. Kolb, and L.-T. Wang, *Phys. Rev. D* **88**, 063510 (2013).
- [51] V. Khachatryan *et al.* (CMS Collaboration), CERN Report No. CMS-PAS-B2G-15-007, 2016.
- [52] G. Aad *et al.* (ATLAS Collaboration), *Eur. Phys. J. C* **75**, 92 (2015).
- [53] A. M. Sirunyan *et al.* (CMS Collaboration), *J. High Energy Phys.* **06** (2018) 027.
- [54] A. M. Sirunyan *et al.* (CMS Collaboration), *Phys. Rev. Lett.* **122**, 011803 (2019).
- [55] V. Khachatryan *et al.* (CMS Collaboration), CERN Report No. CMS-PAS-EXO-16-048, 2017.
- [56] A. M. Sirunyan *et al.* (CMS Collaboration), *Phys. Rev. D* **98**, 032005 (2018).
- [57] W. Buchmuller, R. Ruckl, and D. Wyler, *Phys. Lett. B* **191**, 442 (1987); **448**, 320 (1999).
- [58] W. Buchmuller and D. Wyler, *Phys. Lett. B* **177**, 377 (1986).
- [59] S. Davidson, D. C. Bailey, and B. A. Campbell, *Z. Phys. C* **61**, 613 (1994).
- [60] M. Carpentier and S. Davidson, *Eur. Phys. J. C* **70**, 1071 (2010).
- [61] M. Leurer, *Phys. Rev. D* **49**, 333 (1994).
- [62] G. Aad *et al.* (ATLAS Collaboration), *J. High Energy Phys.* **08** (2016) 009.
- [63] M. Aaboud *et al.* (ATLAS Collaboration), *J. High Energy Phys.* **10** (2017) 182.
- [64] A. M. Sirunyan *et al.* (CMS Collaboration), *J. High Energy Phys.* **06** (2018) 120.
- [65] J. Alwall, R. Frederix, S. Frixione, V. Hirschi, F. Maltoni, O. Mattelaer, H. S. Shao, T. Stelzer, P. Torrielli, and M. Zaro, *J. High Energy Phys.* **07** (2014) 079.
- [66] N. D. Christensen and C. Duhr, *Comput. Phys. Commun.* **180**, 1614 (2009).
- [67] A. Alloul, N. D. Christensen, C. Degrande, C. Duhr, and B. Fuks, *Comput. Phys. Commun.* **185**, 2250 (2014).
- [68] C. Degrande, *Comput. Phys. Commun.* **197**, 239 (2015).
- [69] A. Alves, for further details see, <http://www.athena.biblioteca.unesp.br/exlibris/bd/cathedra/06-01-2016/000180064.pdf>.
- [70] I. Doršner and A. Greljo, *J. High Energy Phys.* **05** (2018) 126.
- [71] T. Sjostrand, S. Mrenna, and P. Z. Skands, *J. High Energy Phys.* **05** (2006) 026.
- [72] J. de Favereau, C. Delaere, P. Demin, A. Giammanco, V. Lemaitre, A. Mertens, and M. Selvaggi (DELPHES 3 Collaboration), *J. High Energy Phys.* **02** (2014) 057.
- [73] G. L. Fogli, E. Lisi, A. Marrone, D. Montanino, and A. Palazzo, *Phys. Rev. D* **66**, 053010 (2002).
- [74] M. C. Gonzalez-Garcia and M. Maltoni, *Phys. Rep.* **460**, 1 (2008).

- [75] J. de Blas, M. Chala, and J. Santiago, *Phys. Rev. D* **88**, 095011 (2013).
- [76] A. Bessaa and S. Davidson, *Eur. Phys. J. C* **75**, 97 (2015).
- [77] A. Greljo and D. Marzocca, *Eur. Phys. J. C* **77**, 548 (2017).
- [78] S. Davidson, S. Descotes-Genon, and P. Verdier, *Phys. Rev. D* **91**, 055031 (2015).
- [79] J. Blumlein, E. Boos, and A. Kryukov, *Z. Phys. C* **76**, 137 (1997).
- [80] A. Belyaev, O. J. P. Eboli, R. Z. Funchal, and T. L. Lungov, *Phys. Rev. D* **59**, 075007 (1999).
- [81] A. Angelescu, D. Beirevi, D. A. Faroughy, and O. Sumensari, *J. High Energy Phys.* **10** (2018) 183.
- [82] M. J. Baker, J. Fuentes-Martín, G. Isidori, and M. König, *Eur. Phys. J. C* **79**, 334 (2019).
- [83] C. Cornella, J. Fuentes-Martin, and G. Isidori, *arXiv*: 1903.11517.